Check for updates

ROYAL SOCIETY
OF CHEMISTRY

Effects of ZIF-8 MOFs on structure and function of blood components

Jiansheng Lin, [ID] [a] Linghong Huang,[b] Haibo Ou,[a] An Chen,[a] Rong Xiang*[c] and Zonghua Liu*[b]

ZIF-8 MOFs, with their large specific surface area and void volume, unique biodegradability and pH sensitivity, and significant loading capacity, have been widely used as carrier materials for bioactive molecules such as drugs, vaccines and genes. In these applications, ZIF-8 MOFs are usually delivered intravenously. Therefore, it is necessary to know the interaction between ZIF-8 MOFs and blood components, which from this sense is a key factor affecting their delivery effectiveness and biosafety. However, until now there has been no report on the evaluation of hemocompatibility of ZIF-8 MOFs. The lack of biosafety information of ZIF-8 MOFs seriously impedes their clinical applications. In this work, we studied the biosafety of two different sizes of ZIF-8 MOFs, mainly focusing on their *in vivo* and *in vitro* effects on the key components of blood (red blood cells (RBCs), platelets, *etc.*) and the coagulation function. It was found that, *in vitro*, a high concentration of ZIF-8 MOFs could induce RBC aggregation and hemolysis, and prolong the coagulation time. *In vivo*, intravenous administration of 45 mg kg^{-1} ZIF-8 MOFs significantly disturbed the RBC and platelet-related blood routine indexes, as well as coagulation function indexes, but it did not cause significant abnormalities in blood coagulation and tissue structures (heart, liver, spleen, lung, and kidney).

1. Introduction

ZIF-8 MOFs have been widely used in biomedical research, for example as drug carriers,[1–3] gene carriers,[4,5] and vaccine carriers,[6,7] due to their porous structure, biodegradable properties in acidic environments, and high reprocessing performance. It is necessary to study the biosafety of ZIF-8 MOFs before they are used in the clinic. Biocompatibility is one of the major requirements of a material to be considered for biomedical applications.[8–11] Biocompatibility can be defined as the ability of a biomaterial to perform its programmed functionality (*e.g.* drug delivery) without adversely affecting the surrounding tissue or altering homeostasis.[12–14] The key aspect associated with biocompatibility is the manner and the resulting effects of biomaterial interaction with cells.

Overall, the existing knowledge on the biocompatibility of the ZIF-8 MOFs is not consistent.[15–19] For example, Vasconcelos *et al.* did not found significant cytotoxicity of the ZIF-8 MOF crystals loading an anti-cancer drug (doxorubicin) towards three cell lines (NCI-H292; HT-29; and HL-60).[20] However, Tamames-Tabar *et al.*[16] observed that the half maximum inhibitory concentrations (IC50) of ZIF-8 MOF on HeLa and J774 cells were 100 and 25 μg mL^{-1}, respectively. Nowadays, although the research on the

biocompatibility of ZIF-8 MOFs is becoming increasingly popular, there are few reports on the interaction of ZIF-8 MOFs with blood.

In light of the above analysis, a comprehensive research to understand and evaluate the biocompatible characteristics of the ZIF-8 MOFs is necessary, which is crucial for their therapeutic applications *in vivo*.[21] As biomedical materials often administered intravenously, ZIF-8 MOFs will inevitably contact with blood. For example, as drug carriers, ZIF-8 MOFs directly enter the blood circulation through intravenous administration, and interact with blood components. This would cause functional changes of blood components, and even alter the function of other organs, thereby affecting their delivery effect and clinical applications.

In this study, the biosafety of two different sizes of ZIF-8 MOFs (80 and 300 nm) was studied. The effects of the ZIF-8 MOFs were evaluated on blood components (red blood cells (RBCs), platelets, *etc.*), coagulation function, and key tissues (heart, liver, spleen, lung, and kidney). Then, the safe concentration and dose ranges of the ZIF-8 MOFs were obtained, and their mechanisms of action were clarified. The results of this study are helpful to deepen the understanding of the effect of ZIF-8 MOFs on cell membrane and platelet activation, and provide useful data for the optimization and further research and application of ZIF-8 MOFs.

2. Materials and methods

2.1. Materials

For the *in vitro* studies, fresh whole blood was obtained from healthy volunteers. All animal experiments were conducted in accordance

a Department of Anatomy, Hunan University of Chinese Medicine, Changsha, 410208, China

b Department of Biomedical Engineering, Jinan University, Guangzhou, 510632, China. E-mail: tliuzonghua@jnu.edu.cn

c Pediatrics Department of Changsha Hospital for Maternal & Child Health Care, Changsha 410007, China. E-mail: 253845188@qq.com

with the Guiding Principles for Animal Care and Use of Hunan University of Chinese Medicine. SD rats were purchased from the laboratory animal center of our university. The ZIF-8 MOFs were synthesized by this study. As show in Fig. 1, the morphology of ZIF-8 MOFs were observed with a scanning electron microscope (Zeiss Ultra 55, Zeiss, Germany). Fig. 1A shows the ZIF-8 MOF (80 nm), and Fig. 1B shows the ZIF-8 MOF (300 nm).

2.2. Methods

2.2.1. Fabrication of ZIF-8 nanocrystals. Firstly, the 2 g of $Zn(NO_3)_2 \cdot 6H_2O$ and 2 g of 2-methylimidazole were stirred in 50 mL of deionized water at 600 rpm for 30 min, and then centrifuged (4000 rpm, 5 min). The precipitate and supernatant were collected. Then the precipitate was washed four times with alcohol and deionized water to obtain the ZIF-8 (300 nm). And
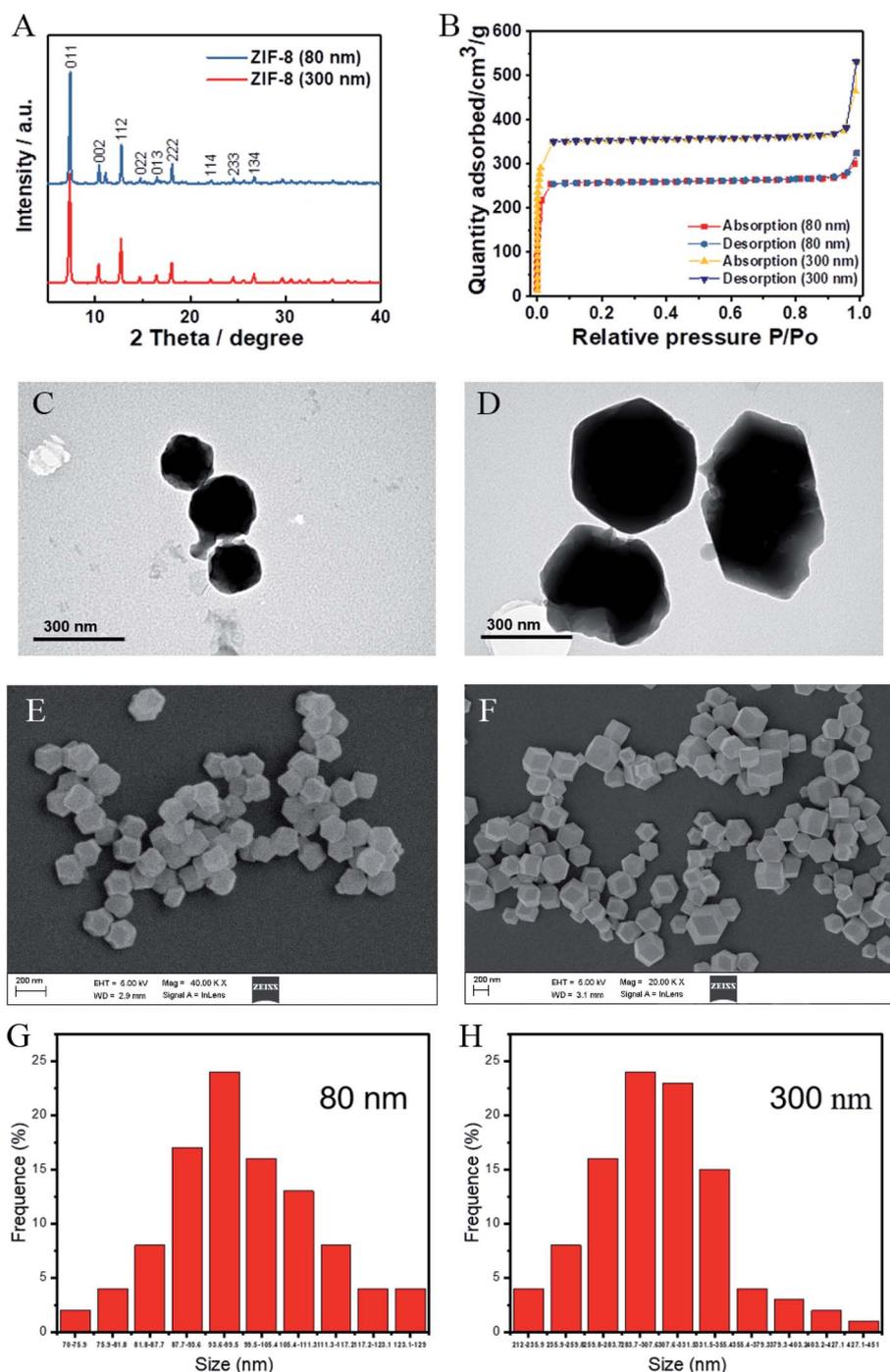

Fig. 1 Physicochemical characterizations of ZIF-8 MOFs. (A) The XRD patterns of ZIF-8 MOFs; (B) the nitrogen adsorption−desorption curves of ZIF-8 MOFs; the TEM observation of (C) ZIF-8 (80 nm) and (D) ZIF-8 (300 nm); (E) the SEM observation of and (G) the corresponding size distribution of ZIF-8 (80 nm); (F) the SEM observation of and (H) the corresponding size distribution of ZIF-8 (300 nm).

the supernatant was centrifuged (12 000 rpm, 10 min), and washed four times with alcohol and deionized water to obtain the ZIF-8 (80 nm). Finally, these two kinds of obtained particles were freeze-dried, and preserved at room temperature.

2.2.2. Characterization of ZIF-8 nanocrystals. The morphological characteristics of ZIF-8 MOFs were observed with scanning electron microscope (SEM, Zeiss, Germany) and transmission electron microscope (TEM, JEM-2010HR, Japan). After the crystals were dried and pressed into tablets, the XRD pattern detection of which was detected with an X-ray powder diffractometer (Miniflex 600, Rigaku, Japan). The specific surface area detection: first, 100 mg ZIF-8 crystals were vacuum degassed at 200 °C for 12 h, and then their specific surface areas were detected with a specific surface area and porosity analyzer (ASAP 2460, Micromeritics, American).

2.2.3. Effects of ZIF-8 MOFs suspension on RBCs morphology and hemolysis

2.2.3.1. RBCs morphology. The fresh healthy human whole blood was centrifuged at $1000 \times g$ for 5 min. After removing the plasma, the RBCs were washed with saline. Then, the RBCs were added to 1 mL of ZIF-8 MOFs suspension of different concentrations, incubated for 30 min at room temperature, and fixed with 4% paraformaldehyde for 2 h. The fixed RBCs were deposited on glass slides, dehydrated with 70, 85, 95, 100% (v/v) ethanol, coated with gold, and observed with a scanning electron microscope (FEI QUANTA 200, Holland).

2.2.3.2. RBCs hemolysis. Fresh RBCs suspension (50 μL, concentration of 16% v/v in saline) were incubated with 1 mL of different concentrations of ZIF-8 MOFs suspension at room temperature. At each preset incubation time point, the suspensions were centrifuged at $1000 \times g$ for 5 min to remove the precipitate. The resulting liquid (200 μL) was loaded into a 96-well plate. The absorbance value (absorption wavelength of 540 nm) was detected with a multifunctional microplate reader (spark, TECAN Corporation, Austria). The positive control was the 100% hemolysis group, and the negative control group was used as blank control. The hemolysis in the presence of the ZIF-8 MOFs was calculated by comparing the absorbance values of the positive control.

2.2.4. Effect of ZIF-8 MOFs suspension on coagulation function

2.2.4.1. Plasma coagulation. The four indexes observed in test for plasma coagulation function include prothrombin time (PT), activated partial thromboplastin time (APTT), fibrinogen (Fib) and thrombintime (TT). The fresh healthy human whole blood anticoagulated by sodium citrate was centrifuged at $1000 \times g$ for 10 min. The supernatant was collected to obtain platelet-poor plasma. Platelet-poor plasma (450 μL) was mixed with 50 μL of ZIF-8 MOFs suspension at different concentrations to obtain the mixture with concentration of 0.01, 0.1 and 1 mg mL^{-1}. The platelet-poor plasma incubated with saline was used as a normal control. The blood clot solidification times of each group of 4 samples were detected on the automatic coagulometer (Sysmex Company, Japan), and the ATPP value, PT value, FIB value and TT value were recorded.

2.2.4.2. Detection of thromboelastogram (TEG). The 900 μL of fresh healthy human whole blood was anticoagulated by sodium citrate, and then mixed with 100 μL of ZIF-8 MOFs suspension with different concentrations, was incubated for 30 min at room temperature. Then, 340 mL of the blood/ZIF-8 MOFs suspension mixture was added to TEG cup. The TEG analysis was initiated by the addition of 20 μL of CaCl$_2$ solution, using the Thromboelastograph Hemostasis System 5000 (Haemoneticse corporation, CFMS LEPU-8880, SUA).

2.2.5. Effect of injecting ZIF-8 MOFs suspension on coagulation function

2.2.5.1. The test of plasma coagulation. SD rats (240 ± 20 g, half male and half female) were randomly divided into seven groups with four in each group. After feeding normally for a week, each rat in the experimental group was injected 500 μL ZIF-8 MOFs suspension with different concentrations through the tail vein. After 30 minutes, the blood was taken from the abdominal aorta of rats and collected in sodium citrate anticoagulant tube. The blood was checked with automatic coagulation analyzer (STARevolution, Diagnostica Stago, France). Then, the results of ATPP, PT, FIB and TT were recorded. After that, the rats injected with 500 μL normal saline were regarded as control group.

2.2.5.2. Test of TEG. SD rats (230 ± 20 g) were randomly divided into seven groups with four in each group. After feeding normally for a week, each rat in the experimental group was injected 500 μL ZIF-8 MOFs suspension with different concentrations through the tail vein. After 30 minutes, the whole blood was taken from the rats with the sodium citrate anticoagulant tube. Then 340 μL fresh whole blood of rats was placed in the test cup and 20 μL CaCl$_2$ was added into the cup. The cup was checked by TEG. After that, the rats injected 500 μL normal saline were regarded as control group.

2.2.6. Effects of injecting ZIF-8 MOFs suspension on blood routine and organs in mice

2.2.6.1. Routine blood test of rats. SD rats (230 ± 20 g, half male and half female) were randomly divided into seven groups with four in each group. After feeding normally for a week, each rat in the experimental group was injected different doses of ZIF-8 MOFs suspension through the tail vein. After 24 h, the whole blood was taken from the rats with EDTA anticoagulant tube, the rats injected 500 μL normal saline were regarded as control group. The 2 mL fresh whole blood of rats was tested by a coagulation analyzer (STAR evolution, Diagnostica Stago, France). The rats injected 500 μL normal saline were regarded as control group.

2.2.6.2. Tissue and organ. SD rats (230 ± 20 g) were randomly divided into seven groups with four in each group. After feeding normally for a week, each rat in experimental group was injected different doses of ZIF-8 MOFs suspension through the tail vein. The doses were 5, 25 and 45 mg kg^{-1}, respectively. After 24 h, the heart, liver, spleen, lung, kidney and brain of each rat in each group were taken out and fixed with 4% paraformaldehyde for 24 h. The tissue sections were made, and H&E staining was performed. The histological structure was observed under microscope (Axioscope 5, ZEISS Corporation, Germany). The rats injected 500 μL of 9% normal saline were regarded as control group.

3. Results and discussion

3.1. Physicochemical characterizations of ZIF-8 MOFs

The crystal structures of the ZIF-8 (80 nm) and ZIF-8 (300 nm) crystals were analyzed by using XRD. As shown in Fig. 1A, the

diffraction peaks of ZIF-8 (80 nm) and ZIF-8 (300 nm) are in good agreement with reported article.[22] The diffraction peaks around $2\theta = 7.35°$, $10.36°$, $12.71°$, $14.70°$, $16.42°$, $18.07°$, $22.12°$, $24.44°$ and $26.70°$ corresponded to the diffraction peaks of the (011), (002), (112), (022), (013) (222), (114), (233) and (134) crystal planes, respectively. In addition, as shown in the Fig. 1B, the results of N_2 adsorption and desorption showed that both ZIF-8 (80 nm) and ZIF-8 (300 nm) had large specific surface areas, which were 1099.48 m^3 g^{-1} and 1497.76 m^3 g^{-1}, respectively. Then, the morphology of ZIF-8 (80 nm) and ZIF-8 (300 nm) were observed by TEM and SEM (Fig. 1C–F), and the results showed that they all have a well-defined rhombic dodecahedral shape, and their corresponding average size results were shown in Fig. 1H and I. It should be mentioned that, once in contact with intra or extracellular media, ZIF-8 MOF is known to suffer disassembly,[7,23,24] and that the liberation of Zn ions could also provoke the effects observed depending on the liberation speed and the concentration of Zn ions, which needs further investigation.

3.2. Effects of ZIF-8 MOFs on RBCs morphology and hemolysis

RBCs are the most abundant blood cells (40–50% blood volume) and have important physiological functions. Biomedical materials used *in vivo* are generally inevitably exposed to blood and often interact with a large number of red blood cells. The interaction between RBCs and biomedical materials can be used to evaluate the safety of biomaterials.[25,26] The normal mature RBCs show bioconcave disc shape, and the erythrocyte membrane is extremely sensitive to the influence of external substances. As a result, the RBC morphology is easily changed by the presence of external substances.[27–29]

First, we investigated the effect of ZIF-8 MOFs on RBCs morphology and aggregation. The results are shown in Fig. 1A. Compared with normal RBCs, the 0.1 mg mL^{-1} ZIF-8 MOFs suspension treated RBCs showed intact cell membrane, clear boundary and normal cell morphology. Nevertheless, the 1 and 10 mg mL^{-1} ZIF-8 MOFs suspensions treated RBCs aggregated and adhered to each other. Therefore, we speculate that because of the strong adsorption of ZIF-8 MOFs, high concentration of ZIF-8 MOFs leaded to RBCs aggregation by adsorbing RBCs, and caused the change of RBCs morphology. Besides, the ZIF-8 MOFs surface has positive charge and the RBCs surface has negative charge, which will produce their electrostatic adsorption. Hence, ZIF-8 MOFs at high concentrations will result in RBCs aggregation and morphological changes.

Furthermore, hemolysis ratio is an important index to reflect the degree of destruction of RBCs membrane, and is often used to study interactions between biomaterials and RBCs. In this work, we studied the effects of different concentrations of ZIF-8 MOFs on hemolysis, as shown in Fig. 1B & C. As shown in Fig. 1B, when 0.1 mg mL^{-1} ZIF-8 MOFs were incubated with
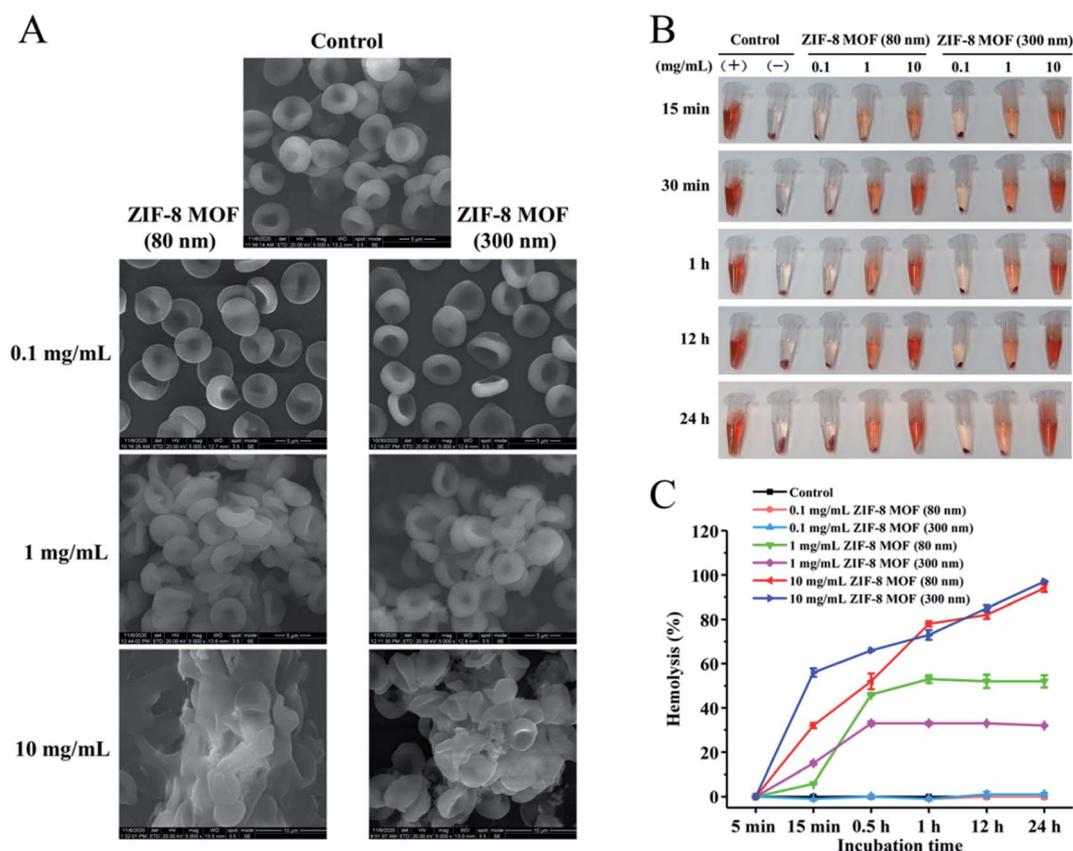

Fig. 2 Effect of the ZIF-8 MOFs on the morphology and hemolysis of RBCs: (A) SEM observation of the RBCs, (B) of the RBCs treated with different concentrations of the ZIF-8 MOFs at room temperature, (C) and hemolysis ratio (means ± SD, $n = 4$).

RBCs for 24 h, no obvious hemolysis was observed. When 1 and 10 mg mL^{-1} ZIF-8 MOFs were incubated with RBCs for 15 min, we can see obvious hemolysis, and it increased along with time. As shown in Fig. 2C, the hemolysis ratio of 0.1 mg mL^{-1} ZIF-8 MOFs was not different from that of negative control group. However, the hemolysis ratio of both ZIF-8 MOFs at 1 mg mL^{-1} was stable after 1 h, hemolysis of ZIF-8 MOF (80 nm) reached 53%, and hemolysis of ZIF-8 MOF (300 nm) reached 33%. Hemolysis caused by 10 mg mL^{-1} ZIF-8 MOFs increased along with time. Hemolysis ratio of ZIF-8 MOF (80 nm) reached 94%, and the hemolysis of ZIF-8 MOF (300 nm) reached 97%.

According to the results, the hemolysis caused by ZIF-8 MOFs is time- and concentration-dependent. With the increase of material concentration and the prolongation of incubation time, the hemolysis increased gradually. We speculate that the hemolysis caused by ZIF-8 MOFs is due to their adsorption to RBCs membrane, which gradually destroys the integrity of RBCs membrane. Combined with the above results, the ZIF-8 MOFs at 0.1 mg mL^{-1} would not affect the morphology and hemolysis of RBCs. At 1 mg mL^{-1} or higher, however, the ZIF-8 MOFs would cause RBCs aggregation, RBCs membrane rupture and hemolysis. It should be mentioned that, at 1 mg mL^{-1}, ZIF-8 (80 nm) particles seem to have a greater impact on erythrocytes, which could be due to the larger surface area of ZIF-8 (80 nm) than that of ZIF-8 (300 nm). At the same concentration, there are more ZIF-8 (80 nm) particles adsorbing around a single erythrocyte, and as a result ZIF-8 (80 nm) particles have a greater impact on red blood cells.

3.3. Effects of ZIF-8 MOFs on coagulation function (*in vitro*)

3.3.1. Effects of ZIF-8 MOFs on plasma coagulation.
APTT, PT, FIB and TT are the routine examination indexes of plasma coagulation in clinic. The coagulation cascade contains three pathways (endogenous, exogenous and common).[30] APTT refers to the time required to form fibrin clot after adding partial thromboplastin reagent and calcium chloride, indicating the level of endogenous coagulation pathway. PT refers to the time required to form fibrin clot after the addition of tissue prothrombin kinase, indicating the level of exogenous coagulation pathway. FIB mainly reflects the content of fibrinogen. TT mainly reflects the time of fibrinogen conversion to fibrin.

In this study, APTT, PT, FIB and TT were used to evaluate the effects of ZIF-8 MOFs on endogenous and exogenous coagulation pathways, respectively. APTT results are shown in Fig. 3A. The plasma APTT values from 0.01 to 0.1 mg mL^{-1} were within normal range, and they were not significantly different from saline group. The plasma APTT values of 1 mg mL^{-1} ZIF-8 MOF (80 nm) and ZIF-8 MOF (300 nm) were significantly higher than those of normal saline, but the APTT values were still in the normal range. The PT results are shown in Fig. 3B. Compared with the control group, there was no difference in plasma PT values of ZIF-8 MOFs at less than 1 mg mL^{-1}. The trends of FIB and TT results are similar to that of the PT results.

From the results above, it can be seen that the addition of a certain concentration of ZIF-8 MOFs would inhibit plasma coagulation, prolong the solidification time, and show
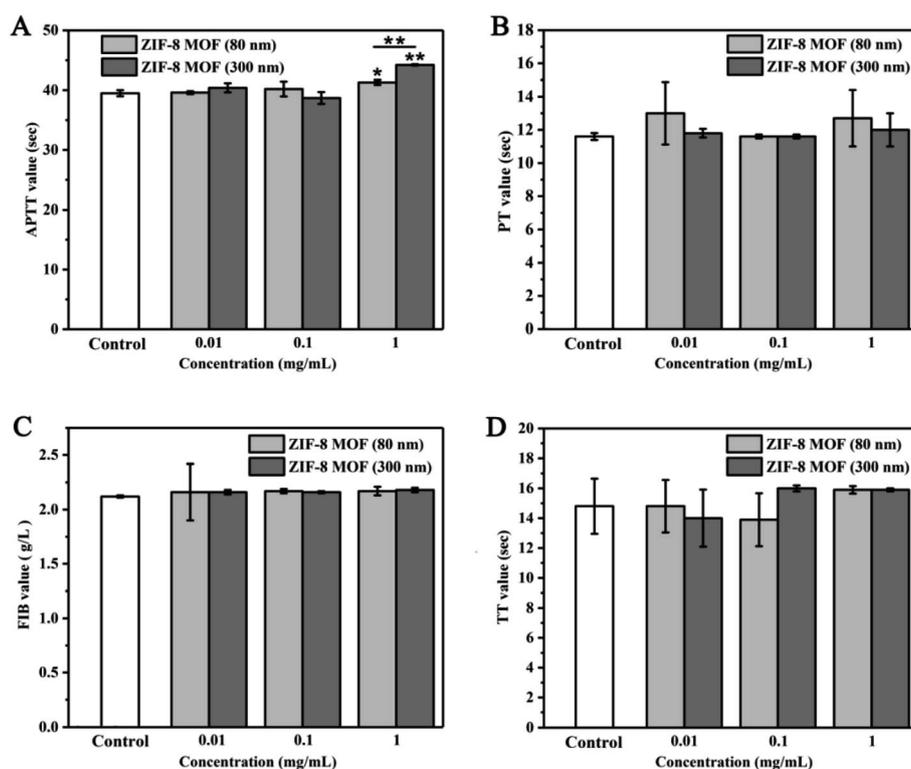

Fig. 3 Effect of ZIF-8 MOFs suspension on coagulation function : (A) APTT values, (B) PT values, (C) FIB values, (D) TT values (>100: the data exceeded the detecting limit of the instrument) (means ± SD, $n = 4$. Statistical significance: *$p < 0.05$, and **$p < 0.05$).
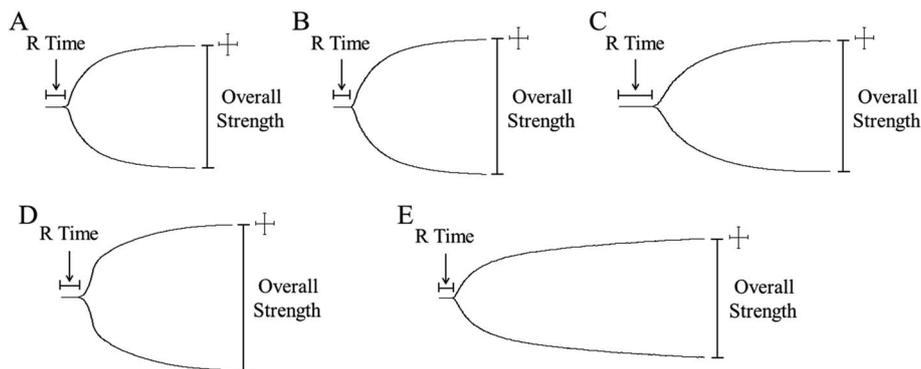
Fig. 4 Representative TEG traces of whole blood coagulation in the presence of the ZIF-8 MOFs.

concentration-dependence. It may due to the strong adsorption of ZIF-8 MOFs, which adsorb coagulation factors and/or fibrinogen, resulting in a decrease in their content in plasma, thus prolonging the coagulation time.

3.3.2. Effect of ZIF-8 MOFs on whole blood coagulation. Blood coagulation is a synergistic process of various blood components, including coagulation factors, fibrinogen and platelets. TEG can be used to detect the effect of specific coagulation components during the blood coagulation.[31,32] There are four main parameters in the TEG test: reaction time R, indicating the activity of coagulation factor, K and α angle, representing the polymerization activity of fibrinogen, and MA, indicating the aggregation activity of platelets.

In this study, we used TEG to study the effect of ZIF-8 MOFs on the whole blood coagulation process. The TEG traces of whole blood coagulation treated with different concentrations of ZIF-8 MOFs are shown in Fig. 5, and the main coagulation parameters are listed in Table 1. As shown in Fig. 4, in the presence of 0.001 mg mL^{-1} ZIF-8 (80 nm) and 0.1 mg mL^{-1} ZIF-8 (300 nm), the blood clotting curves were similar to the saline group. As the ZIF-8 MOF concentration increases, the TEG curves changed. The clot formation time prolonged, and the intensity was weakened. As shown in Table 1, for 0.001 mg mL^{-1} ZIF-8 MOF (80 nm), the four main parameters of TEG are within normal range. The further concentration increase caused one or more index anomalies in the R, K, α angle and MA. Specifically,
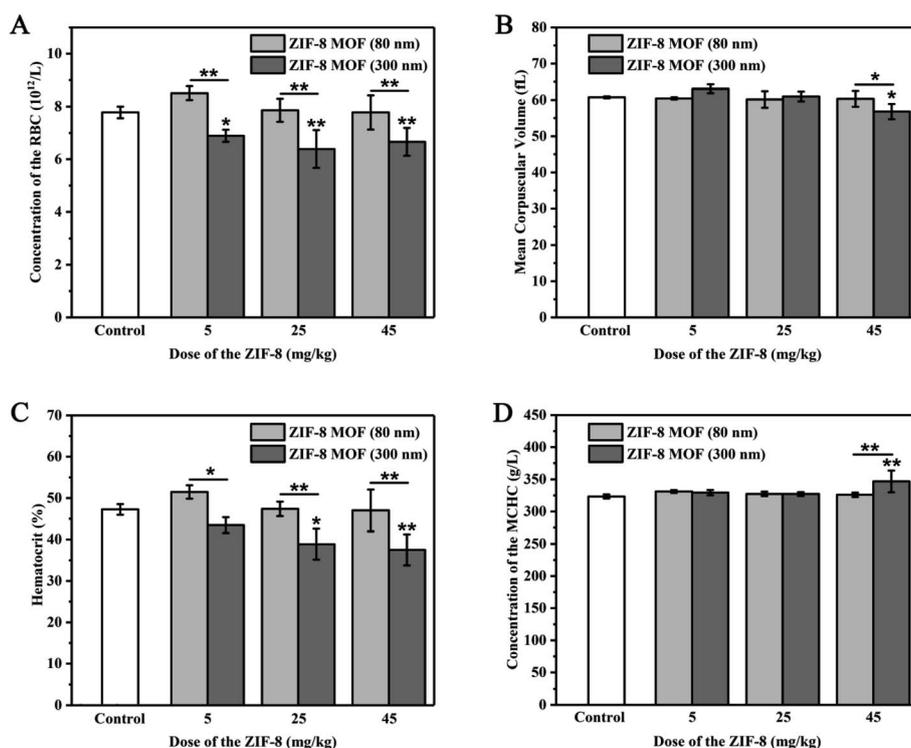

Fig. 5 Effect of the intravenously injected ZIF-8 MOFs on RBCs of the SD rats: (A) RBCs count; (B), Mean Corpuscular Volume (MCV); (C) hemoglobin concentration (HGB); (D), mean corpuscular hemoglobin concentration (MCHC) (means ± SD, $n = 4$. Statistical significance: *$p < 0.05$, and **$p < 0.05$).

Table 1 Clotting kinetics values of human whole blood mixed with ZIF-8 MOFs[a]

ZIF-8 solutions	R (min)	K (min)	α (deg)	MA (mm)
Normal range	5–10	1–3	53–72	50–70
Saline control	6.2	2.1	59.8	55.8
0.001 mg mL^{-1} ZIF-8 MOF (80 nm)	5.3	2.2	64.3	61.0
0.01 mg mL^{-1} ZIF-8 MOF (80 nm)	8.2	4.2↑	44.7↓	50.4
0.1 mg mL^{-1} ZIF-8 MOF (80 nm)	10.4↑	3.7↑	47.9↓	59.1
0.1 mg mL^{-1} ZIF-8 MOF (300 nm)	5.9	2.2	59.8	66.1
0.5 mg mL^{-1} ZIF-8 MOF (300 nm)	4.4↓	3.6↑	54.4	40.6↓
1 mg mL^{-1} ZIF-8 MOF (300 nm)	4.3↓	3.8↑	52.7↓	47.5↓

[a] The sign ↑ indicates a high value and ↓ a low value compared with the normal range provided by the TEG analyzer.

0.01 mg mL^{-1} of ZIF-8 MOF (80 nm) leaded to an increase in the K value, a decrease in α angle, indicating that the addition of ZIF-8 MOF (80 nm) reduced fibrinogen polymerization activity and fibrinogen activity. Addition of 0.1 mg mL^{-1} ZIF-8 MOF (80 nm) resulted in an increase in R values, indicating that coagulation factor activity was inhibited.

However, in the presence of 0.1 mg mL^{-1} of ZIF-8 MOF (300 nm), four main parameters were within the normal range. The addition of 0.5 mg mL^{-1} of ZIF-8 MOF (300 nm) resulted in reduced R, increased K, and reduced MA. We speculate that the addition of ZIF-8 MOF (300 nm) enhanced the activity of coagulation factors, fibrinogen polymerization and platelet aggregation, while fibrinogen activity was not affected. ZIF-8 MOF (300 nm) at 1 mg mL^{-1} leaded to a decrease in α values, which indicates that fibrinogen activity was enhanced.

The results show that the effect of ZIF-8 MOFs on coagulation function was concentration-dependent, that the effect on coagulation components was different, and that the effects of ZIF-8 MOFs on coagulation function varied along with the size of ZIF-8 MOFs. Overall, 0.001 mg mL^{-1} of ZIF-8 MOF (80 nm) and 0.1 mg mL^{-1} ZIF-8 MOF (300 nm) were relatively safe for whole blood coagulation. It is worth noting that, ZIF-8 MOF (80 nm) at 0.1 mg mL^{-1} prolongs the whole blood coagulation, while ZIF-8 MOF (300 nm) at 0.1 mg mL^{-1} does not disturb the whole blood coagulation. It is speculated that, at the same concentration, higher quantity of ZIF-8 MOF (80 nm) and their larger surface area could absorb more coagulation factors and inhibit their activation, thus prolonging the coagulation time.

3.4. Effects of intravenous ZIF-8 MOFs on red blood cells and platelets in rats

Blood routine examination is a commonly used blood detection method in clinic. It is used to detect small changes of various components in blood and can sensitively reflect many pathological changes of the body. In this study, we analyzed the quantity and quality of red blood cells and platelets in the blood by the blood routine examination.

3.4.1. Effects on red blood cells. In blood tests, the parameters reflecting the number and nature of red blood cells include: (1) Red Blood Cell count (RBCs), the number of red blood cells per liter of blood, (2) hemoglobin (HGB), refers to the amount of hemoglobin per liter of blood, (3) hematocrit (HCT), refers to the volume ratio of precipitated red blood cells to total blood after centrifuging a certain amount of anticoagulant whole blood, indirectly reflects the size and volume of red blood cells, (4) Mean Corpuscular Volume (MCV), reflects the average volume of a single red cell, (5) Mean Corpuscular Hemoglobin Concentration (MCHC), refers to average hemoglobin content per liter of red blood cells, its formula is MCV = HCT/RBC. We studied the changes of erythrocyte related indexes in blood routine after intravenously injecting ZIF-8 MOFs.

From Fig. 5, when the ZIF-8 MOF (80 nm) injection dose was 5 to 45 mg kg^{-1}, compared with the control group, RBCs, MCV, HCT and MCHC were not statistically different. When the ZIF-8 MOF (300 nm) injection dose was 5 mg kg^{-1}, compared with the control group, RBCs showed a reduction, MCV, HCT and MCHC were not statistically different. When the ZIF-8 MOF (300 nm) injection dose reached 25 mg kg^{-1}, compared with the control group, it caused a significant reduction of HCT. When the ZIF-8 MOF (300 nm) injection dose increased to 45 mg kg^{-1}, compared with the control group, it resulted in a significant reduction of MCV and a significant increase of MCHC.

Combining with the results of the hemolysis experiments, higher concentrations of ZIF-8 MOF leaded to hemolysis and hemoglobin release. We speculate that *in vivo* injection of high concentrations of ZIF-8 MOF (300 nm) leaded to destruction of the RBCs membrane, and decreased hematocrit, resulting in lower mean corpuscular volume (MCV) and higher mean hemoglobin content (MCHC) values. It is noteworthy that, at 5 mg kg^{-1}, the ZIF-8 (80 nm) particles have a greater impact on erythrocyte amount, which should be due to the larger specific surface area of ZIF-8 (80 nm) particles and a large amount of ZIF-8 (80 nm) particles adsorbing around a single erythrocyte. This result is consistent with those *in vitro* experimental results.

3.4.2. Effects on platelets. The main function of platelets is to clot and stop bleeding and repair damaged blood vessels. The main parameters reflecting platelets in blood routine include: (1) platelet count (PLT), the number of platelets contained in blood per unit volume, (2) Mean Platelet Volume (MPV), the average volume of all platelets in blood and the maturity of platelets, (3) Platelet Volume Ratio (PVR), refers to the percentage of platelets in blood cells, (4) Platelet Distribution Width (PDW), which is a parameter reflecting platelet volume variation in blood.
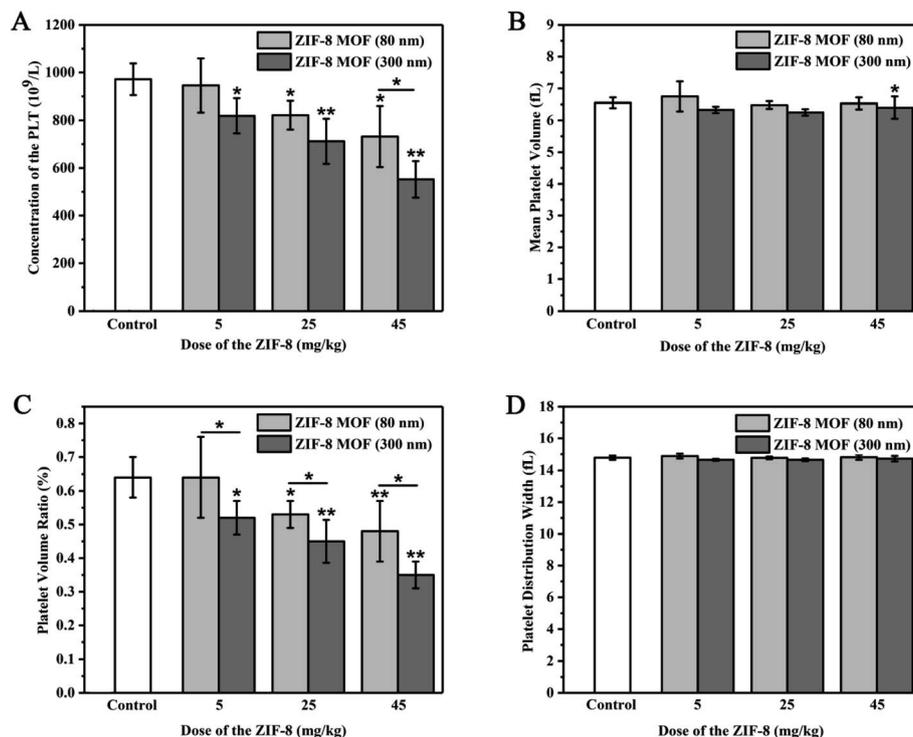
Fig. 6 Effect of the intravenously injected ZIF-8 MOFs on platelet of the SD rats: (A) platelet count (PLT), (B) mean platelet volume (MPV), (C) platelet volume ratio (PVR), (D) platelet distribution width (PDW) (means ± SD, $n = 4$. Statistical significance: *$p < 0.05$, and **$p < 0.05$).

We studied the changes of platelets-related indexes in blood routine after the intravenous injection of ZIF-8 MOFs. As shown in Fig. 6, when the ZIF-8 MOF (80 nm) injection dose was 5 mg kg^{-1}, compared with the control group, PLT, MPV, PVR and PDW had no difference. When the ZIF-8 MOF (80 nm) injection dose was 25 and 45 mg kg^{-1}, compared with the control group, PLT and PVR significantly decreased with the increase of injection dose, and meanwhile there was no difference between PVR and PDW. However, when the ZIF-8 MOF (300 nm) injection dose was from 5 to 45 mg kg^{-1}, compared with the control group, PLT and PVR significantly decreased with the increase of injection dose, and meanwhile there was no difference between PVR and PDW. It is speculated that high concentrations of ZIF-8 MOFs could destroy platelets and reduce platelet count, resulting in a decrease in platelet volume ratio.

3.5. Effects of intravenous ZIF-8 MOFs on coagulation function in rats

3.5.1. APTT, PT, FIB and TT. After the intravenous injection of different doses of ZIF-8 MOFs for 30 min, the APTT, PT, FIB and TT values of plasma coagulation were detected. As shown in Fig. 7, when the injection dose of ZIF-8 MOF (80 nm) was from 5 to 25 mg kg^{-1}, compared with the control group, there was no statistical difference in APTT, PT, FIB and TT values. When the ZIF-8 MOF (80 nm) injection dose increased to 45 mg kg^{-1}, compared with the control group, APTT and TT values significantly increased, and FIB values significantly decreased.

When ZIF-8 MOF (300 nm) injection dose was 5 mg kg^{-1}, there was no significant effect on APTT, PT, FIB and TT values

compared with the control group. When the injection dose of ZIF-8 MOF (300 nm) reached 25 mg kg^{-1}, the APTT value increased compared with the control group. When the injection dose of ZIF-8 MOF (300 nm) reached 45 mg kg^{-1}, the APTT value increased further and the PT value significantly increased compared with the control group.

Therefore, it is speculated that injection of large doses of ZIF-8 MOFs may inhibit blood coagulation in a short period of time, which may be due to the decrease of free coagulation factors and fibrinogen content in blood by ZIF-8 MOFs strong adsorption of plasma proteins.

3.5.2. TEG. The changes of whole blood coagulation were detected by TEG after intravenous injection of ZIF-8 MOFs for 30 min. The effects of ZIF-8 MOFs of different injection doses on the TEG traces of whole blood coagulation are shown in Fig. 8, and the main parameters are listed in Table 2. The blood coagulation TEG curves are similar to that of the control group in the range of 5–45 mg kg^{-1}, as shown in the Fig. 8. There is no statistical difference between the four main TEG parameters and the control group, as shown in Table 2. The results show that, when the injection dose of ZIF-8 MOFs was as high as 45 mg kg^{-1}, there was no obvious effect on whole blood coagulation *in vivo*.

3.6. Effects of ZIF-8 MOFs on tissues and organs of the mice

The pathological changes of tissues or organs can cause changes in blood composition, because the physiological functions of tissues and organs are closely related to those of blood. To be specific, the heart is a power pump of blood
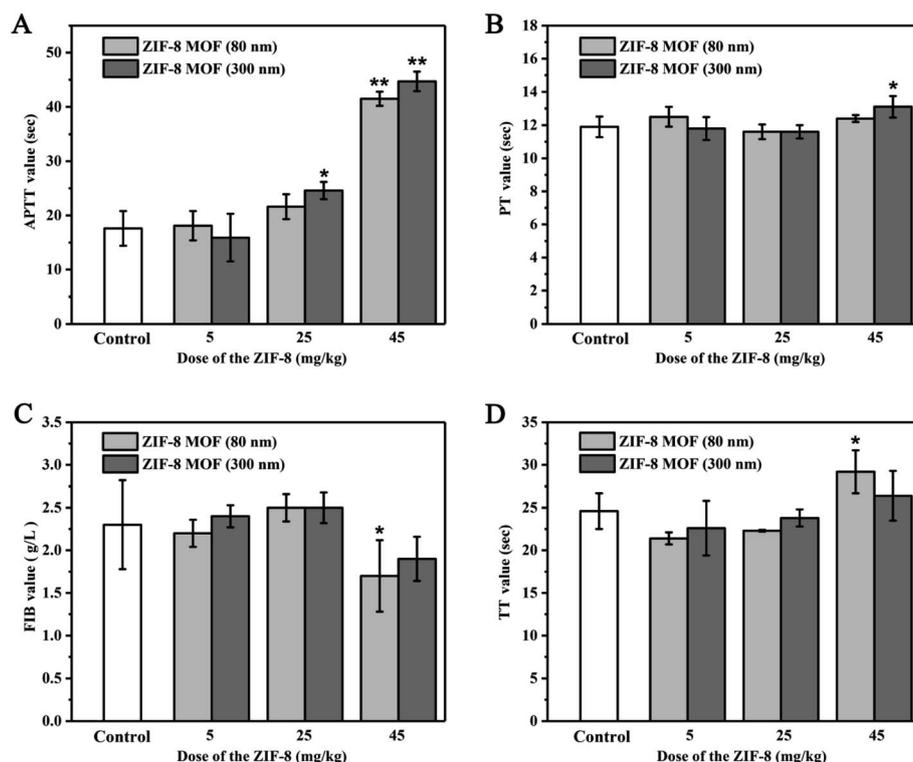
Fig. 7 Effect of the intravenously injected ZIF-8 MOFs particles on coagulation function of the SD rats: (A) APTT values, (B) PT values, (C) FIB values, (D) TT values (>100: the data exceeded the detecting limit of the instrument) (means $\pm$ SD, $n = 4$. Statistical significance: $*p < 0.05$, and $**p < 0.05$).
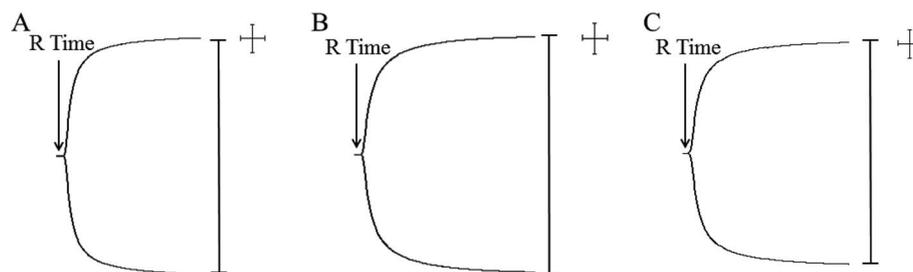

Fig. 8 Representative TEG traces of whole blood coagulation of the SD rats intravenously injected ZIF-8 MOFs.

circulation, and it can affect the physiological functions and components of blood, and *vice versa* changes of blood can also affect the functions of the heart.[33] The liver, which is the main hemopoietic organ in one's embryonic time, is replaced by bone marrow in adulthood, and its hematopoietic function ceases, but it will be restored in some pathological conditions.[34] Besides, nearly all blood coagulation factors are produced by the liver, and it plays a very important role in regulating the

Table 2 Clotting kinetics values of SD-mouse whole blood after injecting ZIF-8 MOFs *in vivo*

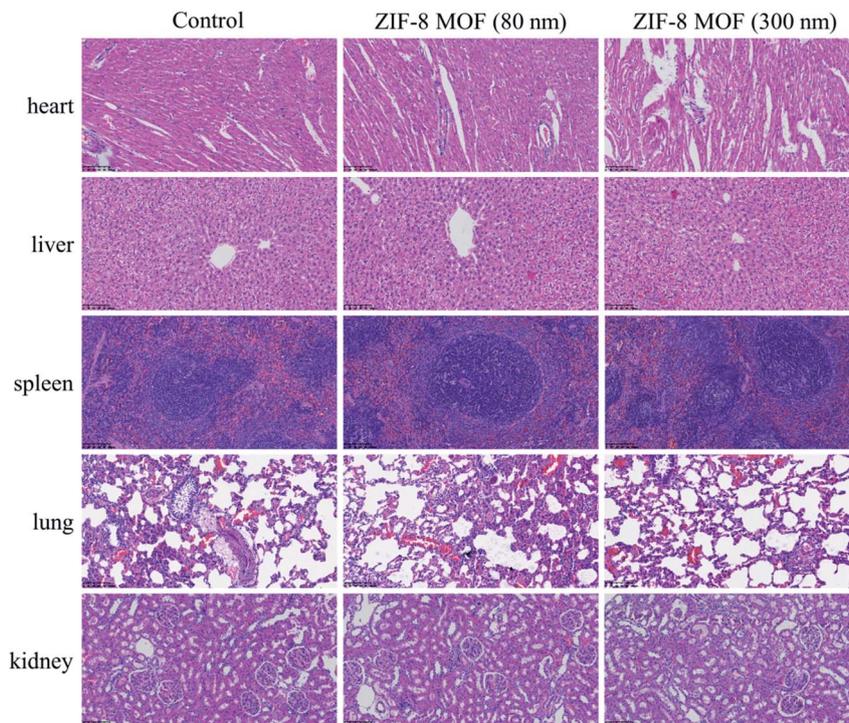| Samples	M (min)	K (min)	α (deg)	MA (mm)
Control	1.53 ± 0.23	0.8 ± 0.00	82.9 ± 1.57	85.2 ± 1.59
5 mg kg^{-1} ZIF-8 MOF (80 nm)	1.47 ± 0.38	0.8 ± 0.00	79.8 ± 1.25	80.4 ± 2.29
5 mg kg^{-1} ZIF-8 MOF (300 nm)	1.47 ± 0.29	0.8 ± 0.00	83.0 ± 1.25	77.0 ± 9.9
25 mg kg^{-1} ZIF-8 MOF (80 nm)	1.53 ± 0.25	0.8 ± 0.00	80.9 ± 1.25	78.7 ± 5.53
25 mg kg^{-1} ZIF-8 MOF (300 nm)	1.53 ± 0.23	0.8 ± 0.00	80.0 ± 2.48	79.9 ± 3.90
45 mg kg^{-1} ZIF-8 MOF (80 nm)	1.57 ± 0.15	0.8 ± 0.00	81.6 ± 1.13	81.6 ± 2.05
45 mg kg^{-1} ZIF-8 MOF (300 nm)	1.50 ± 0.30	0.8 ± 0.00	81.3 ± 2.77	80.3 ± 3.08

Fig. 9 H&E stained tissue sections of the key organs of the SD rats intravenously injected with the ZIF-8 MOFs (scale bar = 100 μm).

dynamic balance of human coagulation and anticoagulation systems. Also, the spleen acts as an important filter in blood circulation, removing foreign bodies, bacteria, and aging and dead cells from the blood, especially RBSs and platelets.[35] The spleen is called the "blood bank" of the human body.[36] When the body is at rest and quiet, the spleen stores blood. However, when it is in a state of stress such as exercise, blood loss and hypoxia, the spleen distributes blood to the blood circulation to increase blood volume. Although the lung is not a hemopoietic organ, it is also involved in the formation of platelets.[18] Last, the kidney generates erythropoietin (EPO) which acts on the bone marrow hematopoietic system to promote the differentiation and maturation of pronormoblasts, facilitate the uptake and utilization of Fe in bone marrow, accelerate the generation of hemoglobin and erythrocyte, and promote the release of bone marrow reticulocytes into blood.[37] As mentioned above, therefore, it is necessary to make intensive research on the effect of ZIF-8 MOFs on these tissues and organs when they enter the blood, and to make further evaluation of blood compatibility of ZIF-8 MOFs *in vivo*.

In this study, the effect of intravenous injection of 45 mg kg^{-1} ZIF-8 MOFs on the above tissue structures was observed through H&E staining, and the results are shown in Fig. 9. Compared with the control group, the characteristics of histological structure of the tested groups are as follows: first, myocardial striations are clear; among the basic structural units of the liver, the structures of central vein, hepatic cord, hepatic sinusoid, perisinusoidal space and bile duct are clearly seen; the structures of capsule and trabecula, white pulp, red pulp and marginal zone in parenchyma of the spleens are clearly

observed; the alveolar duct, alveolar sac, alveolar pore and alveolar septum are clearly seen in the lungs. In general, in the above tissue structures, the cell membrane is intact, and there is no cell edema, no organelle disintegration and other pathological phenomena. In the tissues, the perivascular tissue structures are clearly seen, and there is no inflammatory cell infiltration and immune complex deposition.

Therefore, a preliminary conclusion can be drawn that when the intravenous dose of ZIF-8 MOFs was less than or equal to 45 mg kg^{-1}, they did not cause pathological changes and necrosis of the organs. Combined with the above results, it is supposed that, in a short period of time, the effect of ZIF-8 MOFs on blood would not further cause pathological changes of the organs, the pathological changes of blood were not caused by the damaged organs, and that short-term changes of blood would not cause pathological changes of the organs.

4. Conclusion

In summary, *in vitro* experiments, it is found that the concentration of ZIF-8 MOFs at 0.1 mg mL^{-1} did not cause changes in the morphology and hemolysis of red blood cells, nor did it affect the values of APTT, PT, FIB and TT in coagulation function. And 0.001 mg mL^{-1} ZIF-8 MOF (80 nm) and 0.1 mg mL^{-1} ZIF-8 MOF (300 nm) were relatively safe concentrations for whole blood coagulation. *In vivo* experiments, it is found that, after 30 min, the intravenous dose of ZIF-8 MOFs less than or equal to (≤) 45 mg kg^{-1} did not affect the indicators of whole blood coagulation. When the injection dose of ZIF-8 MOFs was less than or equal to (≤) 5 mg kg^{-1}, it did not affect all

indicators of coagulation function, but with the increase of the injection dose, it would affect one or more indicators of APTT, PT, FIB and TT. When the injection dose of ZIF-8 MOF (80 nm) was 5 mg kg^{-1}, it did not exert effect on platelet indices, but with the increase of the injection dose, it would affect one or more indices of platelet and show a concentration-dependent manner. However, when ZIF-8 MOF (300 nm) was injected at doses between 5 and 45 mg kg^{-1}, it affected one or more platelet indicators and showed a concentration-dependent manner. When the injection dose was less than or equal to ($\leq$) 45 mg kg^{-1}, 24 h after injection, it would not cause any tissue damage to the heart, liver, spleen, lung and kidney. It could be hypothesized that the above changes in blood composition and function were caused by the strong adsorption of ZIF-8 MOFs to cell membrane and plasma proteins.

Conflicts of interest

The authors declare that they have no known competing financial interests or personal relationships that could have appeared to influence the work reported in this paper.

Ethical statement

All animal procedures were performed in accordance with the Guidelines for Care and Use of Laboratory Animals of "Hunan University of Chinese Medicine" University and approved by the Animal Ethics Committee of "Hunan University of Chinese Medicine".

Acknowledgements

References

1 D. F. Sava Gallis, K. S. Butler, J. O. Agola, C. J. Pearce and A. A. McBride, Antibacterial Countermeasures *via* Metal-Organic Framework-Supported Sustained Therapeutic Release, *ACS Appl. Mater. Interfaces*, 2019, **11**(8), 7782–7791.

2 H. Ranji-Burachaloo, A. Reyhani, P. A. Gurr, D. E. Dunstan and G. G. Qiao, Combined Fenton and starvation therapies using hemoglobin and glucose oxidase, *Nanoscale*, 2019, **11**(12), 5705–5716.

3 W. H. Chen, G. F. Luo, M. Vazquez-Gonzalez, R. Cazelles, Y. S. Sohn, R. Nechushtai, Y. Mandel and I. Willner, Glucose-Responsive Metal-Organic-Framework Nanoparticles Act as "Smart" Sense-and-Treat Carriers, *ACS Nano*, 2018, **12**(8), 7538–7545.

4 X. Cao, J. Xia, X. Meng, J. Xu, Q. Liu and Z. Wang, Stimuli-Responsive DNA-Gated Nanoscale Porous Carbon Derived from ZIF 8, *Adv. Funct. Mater.*, 2019, **29**(34), 1902237.

5 H. Wang, Y. Chen, H. Wang, X. Liu, X. Zhou and F. Wang, DNAzyme-Loaded Metal-Organic Frameworks (MOFs) for Self-Sufficient Gene Therapy, *Angew Chem. Int. Ed. Engl.*, 2019, **58**(22), 7380–7384.

6 M. A. Luzuriaga, R. P. Welch, M. Dharmarwardana, C. E. Benjamin, S. Li, A. Shahrivarkevishahi, S. Popal, L. H. Tuong, C. T. Creswell and J. J. Gassensmith, Enhanced Stability and Controlled Delivery of MOF-Encapsulated Vaccines and Their Immunogenic Response In Vivo, *ACS Appl. Mater. Interfaces*, 2019, **11**(10), 9740–9746.

7 Y. Zhang, F. Wang, E. Ju, Z. Liu, Z. Chen, J. Ren and X. Qu, Metal-Organic-Framework-Based Vaccine Platforms for Enhanced Systemic Immune and Memory Response, *Adv. Funct. Mater.*, 2016, **26**(35), 6454–6461.

8 M. Adabi, M. Naghibzadeh, M. Adabi, M. A. Zarrinfard, S. S. Esnaashari, A. M. Seifalian, R. Faridi-Majidi, H. Tanimowo Aiyelabegan and H. Ghanbari, Biocompatibility and nanostructured materials: applications in nanomedicine, *Artif. Cells, Nanomed., Biotechnol.*, 2017, **45**(4), 833–842.

9 M. F. Maitz, C. Sperling, T. Wongpinyochit, M. Herklotz, C. Werner and F. P. Seib, Biocompatibility assessment of silk nanoparticles: hemocompatibility and internalization by human blood cells, *Nanomedicine*, 2017, **13**(8), 2633–2642.

10 L. Xu, M. Kwak, W. Zhang, P. C.-W. Lee and J.-O. Jin, Time-dependent effect of *E. coli* LPS in spleen DC activation in vivo: alteration of numbers, expression of co-stimulatory molecules, production of pro-inflammatory cytokines, and presentation of antigens, *Mol. Immunol.*, 2017, **85**, 205–213.

11 28-Methods for the measurement of cell and tissue compatibility including tissue regeneration processes pdf.

12 K. B. Narayanan, H. D. Kim and S. S. Han, Biocompatibility and hemocompatibility of hydrothermally derived reduced graphene oxide using soluble starch as a reducing agent, *Colloids Surf., B*, 2020, **185**, 110579.

13 M. Niinomi, Design and development of metallic biomaterials with biological and mechanical biocompatibility, *J. Biomed. Mater. Res.*, 2019, **107**(5), 944–954.

14 D. F. Williams, On the mechanisms of biocompatibility, *Biomaterials*, 2008, **29**(20), 2941–2953.

15 E. Shearier, P. Cheng, J. Bao, Y. H. Hu and F. Zhao, Surface Defection Reduces Cytotoxicity of Zn(2-methylimidazole)2 (ZIF-8) without Compromising its Drug Delivery Capacity, *RSC Adv.*, 2016, **6**(5), 4128–4135.

16 C. Tamames-Tabar, D. Cunha, E. Imbuluzqueta, F. Ragon, C. Serre, M. J. Blanco-Prieto and P. Horcajada, Cytotoxicity of nanoscaled metal-organic frameworks, *J. Mater. Chem. B*, 2014, **2**(3), 262–271.

17 T. Wang, S. Li, Z. Zou, L. Hai, X. Yang, X. Jia, A. Zhang, D. He, X. He and K. Wang, A zeolitic imidazolate framework-8-based indocyanine green theranostic agent for infrared fluorescence imaging and photothermal therapy, *J. Mater. Chem. B*, 2018, **6**(23), 3914–3921.

18 L. R. de Moura Ferraz, A. Tabosa, D. D. S. da Silva Nascimento, A. S. Ferreira, V. de Albuquerque Wanderley Sales, J. Y. R. Silva, S. A. Junior, L. A. Rolim, J. J. de Souza Pereira and P. J. Rolim-Neto, ZIF-8 as a promising drug delivery system for benznidazole: development,

characterization, *in vitro* dialysis release and cytotoxicity, *Sci. Rep.*, 2020, **10**(1), 16815.

19 P. Chen, M. He, B. Chen and B. Hu, Size- and dose-dependent cytotoxicity of ZIF-8 based on single cell analysis, *Ecotoxicol. Environ. Saf.*, 2020, **205**, 111110.

20 I. B. Vasconcelos, T. G. d. Silva, G. C. G. Militão, T. A. Soares, N. M. Rodrigues, M. O. Rodrigues, N. B. d. Costa, R. O. Freire and S. A. Junior, Cytotoxicity and slow release of the anti-cancer drug doxorubicin from ZIF-8, *RSC Adv.*, 2012, **2**(25), 9437–9442.

21 M. Hoop, C. F. Walde, R. Riccò, F. Mushtaq, A. Terzopoulou, X.-Z. Chen, A. J. deMello, C. J. Doonan, P. Falcaro, B. J. Nelson, J. Puigmartí-Luis and S. Pané, Biocompatibility characteristics of the metal organic framework ZIF-8 for therapeutical applications, *Appl. Mater. Today*, 2018, **11**, 13–21.

22 D. Bagchi, A. Bhattacharya, T. Dutta, S. Nag, D. Wulferding, P. Lemmens and S. K. Pal, Nano MOF Entrapping Hydrophobic Photosensitizer for Dual-Stimuli-Responsive Unprecedented Therapeutic Action against Drug-Resistant Bacteria, *ACS Appl. Bio Mater.*, 2019, **2**(4), 1772–1780.

23 S. H. Pang, C. Han, D. S. Sholl, C. W. Jones and R. P. Lively, Facet-Specific Stability of ZIF-8 in the Presence of Acid Gases Dissolved in Aqueous Solutions, *Chem. Mater.*, 2016, **28**(19), 6960–6967.

24 A. S. Rifaioglu, E. Nalbat, V. Atalay, M. J. Martin, R. Cetin-Atalay and T. Dogan, DEEPScreen: high performance drug-target interaction prediction with convolutional neural networks using 2-D structural compound representations, *Chem. Sci.*, 2020, **11**(9), 2531–2557.

25 D. Zhong, Y. Jiao, Y. Zhang, W. Zhang, N. Li, Q. Zuo, Q. Wang, W. Xue and Z. Liu, Effects of the gene carrier polyethyleneimines on structure and function of blood components, *Biomaterials*, 2013, **34**(1), 294–305.

26 Y. Huang, Y. Zhang, L. Feng, L. He, R. Guo and W. Xue, Synthesis of N-alkylated chitosan and its interactions with blood, *Artif. Cells, Nanomed., Biotechnol.*, 2018, **46**(3), 544–550.

27 J. Ford, Red blood cell morphology, *Int. J. Lab. Hematol.*, 2013, **35**(3), 351–357.

28 N. Mohandas and P. G. Gallagher, Red cell membrane: past, present, and future, *Blood*, 2008, **112**(10), 3939–3948.

29 Y. Zhang, C. Wang, R. Hu, Z. Liu and W. Xue, Polyethylenimine-Induced Alterations of Red Blood Cells and Their Recognition by the Complement System and Macrophages, *ACS Biomater. Sci. Eng.*, 2015, **1**(3), 139–147.

30 S. Li, Z. Guo, Y. Zhang, W. Xue and Z. Liu, Blood Compatibility Evaluations of Fluorescent Carbon Dots, *ACS Appl. Mater. Interfaces*, 2015, **7**(34), 19153–19162.

31 Y. Zhang, J. Cai, C. Li, J. Wei, Z. Liu and W. Xue, Effects of thermosensitive poly(N-isopropylacrylamide) on blood coagulation, *J. Mater. Chem. B*, 2016, **4**(21), 3733–3749.

32 A. E. Schmidt, A. K. Israel and M. A. Refaai, The Utility of Thromboelastography to Guide Blood Product Transfusion, *Am. J. Clin. Pathol.*, 2019, **152**(4), 407–422.

33 U. Muller-Werdan, R. Prondzinsky and K. Werdan, Effect of inflammatory mediators on cardiovascular function, *Curr. Opin. Crit. Care*, 2016, **22**(5), 453–463.

34 N. Van Braeckel-Budimir, S. P. Kurup and J. T. Harty, Regulatory issues in immunity to liver and blood-stage malaria, *Curr. Opin. Immunol.*, 2016, **42**, 91–97.

35 Y. Sugawara, Y. Hayashi, Y. Shigemasa, Y. Abe, I. Ohgushi, E. Ueno and F. Shimamoto, Molecular Biosensing Mechanisms in the Spleen for the Removal of Aged and Damaged Red Cells from the Blood Circulation, *Sensors*, 2010, **10**(8), 7099–7121.

36 M. F. Cesta, Normal structure, function, and histology of the spleen, *Toxicol. Pathol.*, 2006, **34**(5), 455–465.

37 A. T. Layton, H. E. Layton, W. H. Dantzler and T. L. Pannabecker, The mammalian urine concentrating mechanism: hypotheses and uncertainties, *Plant Physiol.*, 2009, **24**, 250–256.